Identification of a Late Stage of Small Noncycling pTα$^-$ Pre-T Cells as Immediate Precursors of T Cell Receptor α/β$^+$ Thymocytes

By César Trigueros,* Almudena R. Ramiro,* Yolanda R. Carrasco,* Virginia G. de Yebenes,* Juan P. Albar,‡ and María L. Toribio*

*From the *Centro de Biología Molecular "Severo Ochoa," and the ‡Departamento de Inmunología y Oncología, Centro Nacional de Biotecnología, Universidad Autónoma de Madrid, Cantoblanco, 28049 Madrid, Spain*

Summary

During thymocyte development, progression from T cell receptor (TCR)β to TCRα rearrangement is mediated by a CD3-associated pre-TCR composed of the TCRβ chain paired with pre-TCRα (pTα). A major issue is how surface expression of the pre-TCR is regulated during normal thymocyte development to control transition through this checkpoint. Here, we show that developmental expression of pTα is time- and stage-specific, and is confined in vivo to a limited subset of large cycling human pre-T cells that coexpress low density CD3. This restricted expression pattern allowed the identification of a novel subset of small CD3$^-$ thymocytes lacking surface pTα, but expressing cytoplasmic TCRβ, that represent late noncycling pre-T cells in which recombination activating gene reexpression and downregulation of T early α transcription are coincident events associated with cell cycle arrest, and immediately preceding TCRα gene expression. Importantly, thymocytes at this late pre-T cell stage are shown to be functional intermediates between large pTα$^+$ pre-T cells and TCRα/β$^+$ thymocytes. The results support a developmental model in which pre-TCR–expressing pre-T cells are brought into cycle, rapidly downregulate surface pre-TCR, and finally become small resting pre-T cells, before the onset of TCRα gene expression.

Key words: pre-T cells • pTα • noncycling • recombination activating gene • T early α

Early in T cell development, thymocytes that have succeeded in productive V-D-J rearrangements at the TCRβ locus are selected for cellular expansion and further maturation before the TCRα gene is expressed (1–3). This process, termed "β-selection," is regulated by the pre-TCR, which comprises the CD3 complex in association with the TCRβ chain and the invariant pre-TCRα (pTα)[1] chain (4–6). A key question has been whether surface expression is essential for the pre-TCR complex to exert its regulatory function. Recent studies support that this may be the case, since pre-TCR–induced thymocyte maturation involves both the extracellular constant region and the transmembrane region of TCRβ (7), and requires exit of the pre-TCR from the endoplasmic reticulum/*cis*-Golgi compartment (8). The question remains as to whether pre-TCR signaling is triggered by binding to an extracellular ligand or, alternatively, as proposed recently (9), whether pre-TCR complexes become constitutively active as soon as they reach the plasma membrane, where signaling molecules are available. In this latter situation, pre-TCR activity might be regulated by control of membrane expression. However, extremely low levels of the pre-TCR complex (~100-fold lower than those of the TCRα/β on mature T cells) appear to reach the plasma membrane of immature thymocytes (10), a fact that has hindered the development of monospecific anti–pre-TCR reagents and, hence, the study of pre-TCR expression patterns on normal thymocytes.

Current data support the notion that one of the first consequences of pre-TCR expression is the induction of a cell cycle progression that results in the greatest expansion in cell numbers that occurs in the developing thymus (1, 11). In mice, this process is associated with differentiation of CD44^{lo}CD25$^+$ into CD44^{lo}CD25$^-$ double negative (DN)

[1]*Abbreviations used in this paper:* DN, CD4$^-$CD8$^-$ double negative; DP, CD4$^+$CD8$^+$ double positive; GFP, green fluorescent protein; PI, propidium iodide; pTα, pre-TCRα; RAG, recombination activating gene; RT, reverse transcription; SP, single positive; TEA, T early α; FSC, forward side scatter; FTOC, fetal thymic organ culture.

C. Trigueros and A.R. Ramiro contributed equally to this work.

 J. Exp. Med. © The Rockefeller University Press • 0022-1007/98/10/1401/12 $2.00
Volume 188, Number 8, October 19, 1998 1401–1412
http://www.jem.org

thymocytes, suggesting that the pre-TCR is first expressed on the cell surface at this developmental transition (11). Accordingly, $CD44^{lo}CD25^{-}$ thymocytes from normal mice are large-sized cells expressing trace but distinguishable levels of TCRβ and CD3 (12). Similarly, the fraction of large thymocytes present in TCRα-deficient mice as well as in TCRβ transgenic recombination activating gene (RAG)-1 mutant mice expresses low but stoichiometric levels of TCRβ and CD3 (13, 14). A highly analogous checkpoint may occur in T cell development in humans during the transition from $CD4^{+}CD8^{-}$ $TCR\alpha/\beta^{-}$ precursors to $CD4^{+}CD8^{+}$ $TCR\alpha/\beta^{-}$ double positive (DP) thymocytes, as the latter cells are mostly large cycling cells, in which TCRβ is part of a complex that is distinct from the mature TCRα/β, and could be the pre-TCR (15).

The pre-TCR–induced cell cycle transition is, in turn, associated with the downregulation of RAG-1 and RAG-2 gene transcription (16) and RAG-2 protein expression (11), which is likely to be an important component of the process of allelic exclusion at the TCRβ locus (3, 11). However, RAG genes have to be reexpressed at a later stage to allow rearrangements at the TCRα locus (16). Likewise, TCRα germline transcription and, hence, expression of sterile T early α (TEA) transcripts, is later induced as an obligatory early event in the opening of the TCRα locus for subsequent VJα rearrangement (17). This terminal program is rapidly triggered in mice during, or immediately after, the transition from $CD44^{lo}CD25^{-}$ cycling thymocytes to $CD4^{+}CD8^{+}$ DP resting thymocytes (16–18). Accordingly, surface expression of the mature CD3–TCRα/β complex is first detectable on small nonproliferating DP thymocytes (19, 20). However, progress towards a more precise definition of the stages involved in the transition from TCRβ to TCRα locus rearrangement has been hampered thus far, both in mice and in humans, because previous attempts to demonstrate surface expression of the pre-TCR complex throughout normal thymocyte development have been unsuccessful.

In this study, analysis performed with a polyclonal rabbit Ab that recognizes an exposed epitope of the native human pTα protein revealed a restricted pattern of surface pTα expression during normal human pre-T cell development. On the basis of surface CD3/pTα expression and cell size, we have identified a novel subset of small pre-T cells which lack surface CD3/pTα expression and are mostly in a noncycling state. Transition to this developmental stage is shown to be associated with the induction of specific developmental events that precede expression of the TCRα gene. Interestingly, such small $pT\alpha^{-}$ noncycling pre-T cells are shown to be functional intermediates between large pTα-bearing pre-T cells and the first thymocytes expressing the mature α/β TCR.

Materials and Methods

Isolation of Thymocyte Subsets. Postnatal thymocytes isolated from thymus samples removed during corrective cardiac surgery of patients aged 1 mo to 3 yr were fractionated by centrifugation on stepwise Percoll density gradients (LKB, Uppsala, Sweden), as described elsewhere (21). Thymocytes from the 1.068 and 1.08 density layers were designated as large and small thymocytes, respectively. Large thymocytes were depleted (>99% purity) of mature T cells (α/β and γ/δ), B cells, NK cells, and myeloid cells by two rounds of treatment with magnetic beads (Dynabeads; Dynal A.S., Oslo, Norway) coupled to the following mAbs: anti-TCRα/β (BMA031 [reference 22]; provided by Dr. R. Kurrle, Behringwerke AG, Marburg, Germany); anti-TCRγ/δ (TCRδ1 [reference 23]; provided by Dr. M. Brenner, Brigham and Women's Hospital, Boston, MA); anti-CD19 (Dynal A.S.), anti-CD56 (Leu-19; Becton Dickinson, San Jose, CA), and anti-CD14 (3C10, TIB 228; American Type Culture Collection, Rockville, MD). $CD4^{+}CD8^{+}$ thymocytes were magnetically sorted from the recovered pool with anti-CD8–coated beads (Dynal A.S.), and $CD4^{+}CD8^{-}CD3^{-}$ thymocytes were then sorted from the CD8-depleted pool with anti-CD4–coated beads (Dynal A.S.), as described (15). Cells in the former subset (referred to as large $TCR\alpha/\beta^{-}$ DP thymocytes) were either $CD3^{-}$ or $CD3^{low}$. Isolation of the $CD3^{-}$ cells (referred to as large $CD3^{-}$ DP thymocytes) was performed by depletion of $CD3^{low}$ cells with anti-CD3–coated magnetic beads (Dynal A.S.). To avoid cell death induced by treatment with anti-CD3, large $CD3^{low}$ DP thymocytes were isolated from the 1.068 fraction recovered after two rounds of fractionation on Percoll gradients, followed by depletion of T, B, NK, and myeloid cells, and anti-CD8 sorting, as described above. Such large $TCR\alpha/\beta^{-}$ DP thymocytes consisted almost entirely (95–99%) of $CD3^{low}$ cells.

Small thymocytes recovered from the 1.08 density layer were depleted of $TCR\alpha/\beta^{+}$ thymocytes (either $CD3^{int}$ or $CD3^{bright}$) by anti-TCRα/β magnetic bead depletion as described above for large cells. $CD3^{-}$ cells (termed small $CD3^{-}$ DP thymocytes) were then isolated from the recovered population (>99% $CD4^{+}CD8^{+}$) by anti-CD3 bead depletion (Dynal A.S.). Mature $TCR\alpha/\beta^{+}$ single positive (SP) thymocytes were isolated as described previously (15).

Flow Cytometry Analysis. Directly labeled mAbs against CD3 (Leu4-PE) and CD8 (Leu2a-FITC) were obtained from Becton Dickinson; anti-CD4 (CD4-PE-Cy5) mAbs were purchased from Caltag Laboratories, Inc. (San Francisco, CA). A PE-labeled mAb against the human TCR $V_{\beta}1$ family (24) was obtained from Serotec Ltd. (Kidlington, Oxford, UK). Unlabeled mAbs against monomorphic determinants of either TCRα/β (BMA031) or TCRγ/δ (TCRδ1), or against the human TCR $V_{\alpha}12.1$ (25; provided by Dr. M. Brenner), were used in combination with goat anti–mouse FITC- or PE-coupled $F(ab')_2$ Ig (Caltag Laboratories, Inc.). Isotype-matched irrelevant mAbs (Caltag Laboratories, Inc.) were used as negative controls.

For detection of cytoplasmic TCRβ, cells were stained with the anti-TCRβ chain mAb βF1 (26; provided by Dr. M. Brenner), as described elsewhere (15). Surface expression of pTα chain was determined by sequential staining with a rabbit polyclonal Ab (ED-1) derived in this study (see below), plus FITC-conjugated goat anti–rabbit $F(ab')_2$ Ig (Southern Biotechnology Associates, Inc., Birmingham, AL). Preimmune rabbit serum was used as negative control. For peptide competition, peptide (100 μg/ml) was first incubated with the anti-pTα serum for 1 h at room temperature. Stained cells were analyzed in a flow cytometer (EPICS XL; Coulter Corp., Hialeah, FL) as described previously (15). Cell cycle analyses were performed by flow cytometry using a doublet discrimination function in cells treated with 0.05% digitonin (Sigma Chemical Co., St. Louis, MO), washed, and stained

with 50 μg/ml of propidium iodide (PI; Sigma Chemical Co.), as described elsewhere (15).

Generation of Polyclonal Anti–human pTα Abs. A synthetic peptide corresponding to the human pTα sequence 61–82 (15), with an additional Cys in the COOH-terminal region, was coupled to Maleimide-activated KLH following the manufacturer's instructions (Pierce Chemical Co., Rockford, IL). Rabbits were immunized with 1 mg of the peptide–KLH conjugate in CFA (Difco Laboratories Inc., Detroit, MI) and boosted 30 and 50 d later with 0.5 mg of immunogen in IFA (Difco Laboratories Inc.). The animals were bled 10 d after the last booster injection, and the sera were purified by affinity chromatography (Sulfolink Coupling gel; Pierce Chemical Co.) and tested for antipeptide reactivity with a horseradish peroxidase–labeled polyclonal goat anti–rabbit IgG (Nycomed Amersham plc, Little Chalfont, Bucks, UK) plus *o*-phenylenediamine dihydrochloride (OPD; Sigma Chemical Co.).

Cell Transfections and Immunofluorescence Assays. C-myc tagging was performed by PCR amplification of a complete pTα cDNA contained in the Bluescript-KS II plasmid (Stratagene Inc., La Jolla, CA) with the sense 5′-GGG CCC GGA TCC ATA TGG CCG GTA CAT GGC TG-3′ and antisense 5′-GGG GGA TCC TCA CAG GTC TTC CTC GGA GAT CAG CTT CTG CTC TCC GCC GGC AGC TCC AGC CTG CAG-3′ primers, which contained the sequence coding for the 9E10 mAb–reacting c-myc peptide. The PCR product was subsequently BamHI digested and ligated into the pSRα vector (pSR-pTαmyc [reference 27]; provided by Dr. B. Alarcón, Centro de Biología Molecular "Severo Ochoa"). The pTα–green fluorescent protein (GFP) fusion was carried out by PCR amplification of a complete pTα cDNA with the sense 5′-GGG CCC GGA TCC ATA TGG CCG GTA CAT GGC TG-3′ and antisense 5′-GGG GGA TCC CCG GCA GCT CCA GCC TGC AG-3′ primers followed by digestion and ligation into the BamHI site of the pEGFP-N1 plasmid vector (Clontech, Palo Alto, CA). An EcoRI-NotI restriction fragment from the pPTα-EGFP vector was subsequently ligated into the pcDNA3 plasmid vector (Invitrogen Corp., Carlsbad, CA). The TCRα ($V_α$12.1) full-length cDNA (AV12S1) was the gift of Dr. J.A. López de Castro (Centro de Biología Molecular "Severo Ochoa"). AV12S1 cDNA (28) was cloned into the BamHI site of the pcDNA3 plasmid vector. COS cells were transfected by electroporation with 5 μg of pSR-pTαmyc plasmid plus 20 μg of carrier pUC-19 plasmid DNA (Promega Corp., Madison, WI), at 250V, 960 μF in a Gene Pulser (Bio-Rad Laboratories, Richmond, CA) as described elsewhere (27). Electroporated cells were then plated on coverslips. SUP-T1 cells were electroporated with 30 μg of the pTα-GFP or AV12S1-containing vectors as described above, and 24–48 h afterwards transfected cells were plated into 96-well round-bottomed plates at 10^5 cells/ml, grown in the presence of 1 mg/ml G418 for 2 wk, and analyzed by flow cytometry.

For immunofluorescence detection, 24–48 h after transfection, COS cells were fixed with 2% paraformaldehyde, washed in PBS, and permeabilized with 0.1% saponin in PBS containing 1% BSA as blocking agent. The coverslips were then sequentially incubated with the 9E10 anti–c-myc mAb (CRL 1729; American Type Culture Collection), the ED-1 anti-pTα rabbit antiserum, FITC-conjugated goat anti–rabbit Ig, and Texas red–conjugated goat anti–mouse $F(ab')_2$ IgG (Southern Biotechnology Associates, Inc.). The coverslips were visualized on a Zeiss Axioskop microscope.

Northern Blot Analysis. Preparations of total RNA (10 μg) isolated as described previously (15) were run on 1% agarose/formaldehyde gels, transferred to nylon membranes, and hybridized with ^{32}P-labeled cDNA probes corresponding to the TCR Cα (PY1.4 [29]) or Cβ (Jurβ$_2$ [30]) regions (provided by Dr. T.W. Mak, The Ontario Cancer Institute, Toronto, Ontario, Canada). The RAG-1 and RAG-2 cDNA probes (31) were the gift of Dr. L.A. Turka (The Howard Hughes Medical Institute, Ann Arbor, MI), and the human pTα cDNA probe was derived in our laboratory (15). The TEA probe was generated by PCR amplification (sense primer 5′-TGG ATG GAT AGA GAC AAG TGC-3′ and antisense primer 5′- CCT GCC CTG GGG AAT AAT AGG-3′) of the K562 erythroleukemia genomic DNA and cloning in a pMOS Blue-T vector (Nycomed Amersham plc). The fragment obtained by HindIII-EcoRI restriction was used for Northern blotting. The same blot was subsequently stripped and hybridized with a β-actin probe (15).

Reverse Transcription PCR Analysis. Total RNA (1 μg) was reverse-transcribed into cDNA according to the manufacturer's protocol (Boehringer Mannheim, Mannheim, Germany). Equivalent amounts of cDNA among different samples was estimated by reverse transcription (RT)-PCR carried out for 18, 21, and 25 cycles with β-actin primers as described previously (15). Titration of cycle number allowed us to perform densitometric analyses (Bio-imaging BAS 1500; Fujifilm, Kanagawa, Japan) under non-saturating conditions. Vα degenerate primers used in combination with Cα primers enabled the amplification of all known human Vα segments, as described (32). Specific amplifications were detected by Southern blotting with a Cα probe (29).

Hybrid Human/Mouse Fetal Thymic Organ Cultures. The in vitro generation of mature TCRα/β$^+$ human T cells was analyzed using a modification of the previously described hybrid human/mouse fetal thymic organ culture (hu/mo FTOC [33]). In brief, thymi removed from 15-d-old embryos of Swiss mice were precultured for 5–6 d in the presence of 1.35 mM dGuo (Sigma Chemical Co.). The thymic lobes were then washed and cocultured in hanging drops in Terasaki plates (Nunc, Inc., Roskilde, Denmark) with either large CD3^{low} (10^5 cells/lobe) or small CD3$^-$ (10^6 cells/lobe) human pre-T cells. After 2 d, lobes were transferred to filters (Millipore Corp., Bedford, MA), which were layered over gelfoam rafts and cultured in IMDM supplemented with 2% human AB serum and 5% FCS (GIBCO BRL, Paisley, UK). Surface staining of human cells was performed at the indicated culture periods, and flow cytometric analyses were then performed on electronically gated CD45$^+$ human cells.

Results

Surface CD3 Expression and Cell Size Define Distinct Subsets of Human TCRα/β$^-$ DP Thymocytes. We have previously identified a subset of large cycling CD4$^+$CD8$^+$ human thymocytes in which the TCRβ chain is expressed as part of a complex distinct from the mature α/β TCR, likely the pre-TCR (15). According to their size, such TCRα/β$^-$ DP thymocytes could be selectively isolated from the fraction of large cells recovered from Percoll density gradients (approximately one third of total unfractionated thymocytes), whereas conventional TCRα/β$^+$ DP thymocytes were more common with the small-sized cell fraction (around two thirds of total thymocytes [15]). Since human thymocytes typically coexpress CD3 and the α/β TCR in stoichiometric amounts, CD3 expression studies similarly defined a differential distribution of cell subsets among Percoll-fractionated thymocytes (Table 1). However, analysis of the correlated expression of CD3 versus

Table 1. *FSC Analysis and Relative Cell Numbers of Human Thymocyte Subsets as Defined by Their CD3 Expression Levels*

Subset	Thymocyte fraction					
	Total thymocytes		Large thymocytes		Small thymocytes	
	relative no. (%) ± SD	*mean FSC ± SD*	*relative no. (%) ± SD*	*mean FSC ± SD*	*relative no. (%) ± SD*	*mean FSC ± SD*
$CD3^-$	22 ± 4.8	357 ± 12.1	28 ± 4.9	358 ± 12.0	19 ± 2.2	333 ± 17.2
$CD3^{low}$	21 ± 4.5	377 ± 14.3	25 ± 5.6	395 ± 19.5	17 ± 2.4	342 ± 22.3
$CD3^{int}$	31 ± 3.4	335 ± 22.3	13 ± 2.7	346 ± 20.0	45 ± 4.6	313 ± 14.3
$CD3^{bright}$	24 ± 4.6	340 ± 11.6	29 ± 5.1	330 ± 12.2	17 ± 6.1	329 ± 11.1

Postnatal thymocytes were fractionated into large and small cells on Percoll density gradients. $CD3^-$, $CD3^{low}$, $CD3^{int}$, and $CD3^{bright}$ subsets from each fraction were analyzed for cell size by flow cytometry (mean FSC ± SD of 10 independent experiments). Unfractionated total thymocytes are included for comparison.

TCRα/β revealed that, although most large TCRα/β$^-$ thymocytes were $CD3^-$, a distinct proportion of them expressed low but detectable levels of CD3 (Fig. 1). These large $CD3^{low}$ TCRα/β$^-$ thymocytes did not represent γ/δ T cells, as expression of the γ/δ TCR was exclusively detected on large TCRα/β$^-$ thymocytes with a $CD3^{bright}$ phenotype (Fig. 1, and data not shown). Unexpectedly, $CD3^-$ and $CD3^{low}$ cells were also recovered from the small cell fraction (Fig. 1). Forward scatter (FSC) analyses ruled out the possibility that such cells represented large-sized contaminants (Table 1). Moreover, in contrast to large $CD3^{low}$ thymocytes, essentially all $CD3^{low}$ small cells (15–20% of total small thymocytes) coexpressed the α/β TCR. However, small $CD3^-$ thymocytes were phenotypically similar to $CD3^-$ large cells in that they expressed neither the α/β nor the γ/δ TCR (Fig. 1, and data not shown). As both large and small $CD3^{low}$ thymocytes displayed a homogeneous $CD4^+CD8^+$ DP phenotype (see below), they were phenotypically indistinguishable except for the expression of α/β TCR on small DP thymocytes, but not on large DP thymocytes.

Surface Expression of pTα Chain Can Be Detected with an Anti-pTα Ab. The above results prompted us to investigate whether large thymocytes with the $CD3^{low}$ TCRα/β$^-$ phenotype do represent pre-T cells expressing the pre-TCR. However, this issue was difficult to approach because no appropriate reagents such as anti-pTα Abs or Abs able to recognize the human TCRβ chain on the cell surface were available. Consequently, Abs were raised in rabbits against a synthetic peptide contained in the extracellular Ig-like domain of the human pTα molecule (15). The specificity of the affinity-purified antisera was then assayed by immunofluorescence microscopy of COS cells transfected with a pTα cDNA, tagged with a c-myc epitope that is recognized by the specific 9E10 mAb. Results in Fig. 2 *A* show that one of these anti-pTα antisera (ED-1) was reactive against all c-myc$^+$ transfectants (*top panels*), and that both anti–c-myc and anti-pTα reagents displayed an identical intracellular recognition pattern (*bottom panels*), thus confirming the anti-pTα specificity of the ED-1 antiserum.

To determine whether the anti-pTα antiserum was also able to recognize the pTα chain when expressed on the cell surface, we next derived pTα stable transfectants from the human T cell line SUP-T1, which expresses TCRβ ($V_{β1.1}$) in the absence of a functional TCRα chain and, hence, lacks surface TCRα/β heterodimers (34). As a

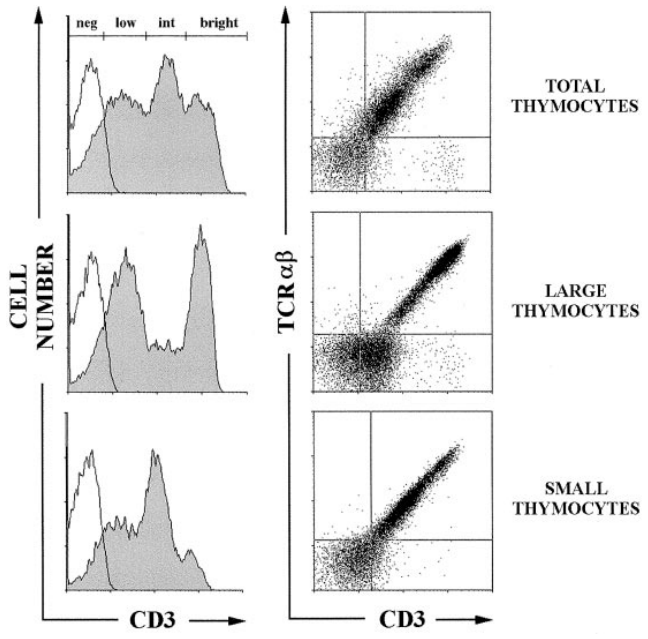

Figure 1. Cell surface phenotype of total and Percoll-fractionated large and small thymocytes. Successive thymocyte differentiation stages characterized by their CD3 expression levels as negative (*neg*), low, intermediate (*int*), and bright are differentially distributed within large- and small-sized Percoll-separated thymocytes (*shaded monoparametric histograms*). Background values were obtained with isotype-matched irrelevant mAbs (*unshaded histograms*). Each thymocyte fraction was analyzed by two-color flow cytometry for the expression of TCRα/β (BMA031) versus CD3. Background values were determined with isotype-matched irrelevant mAbs.

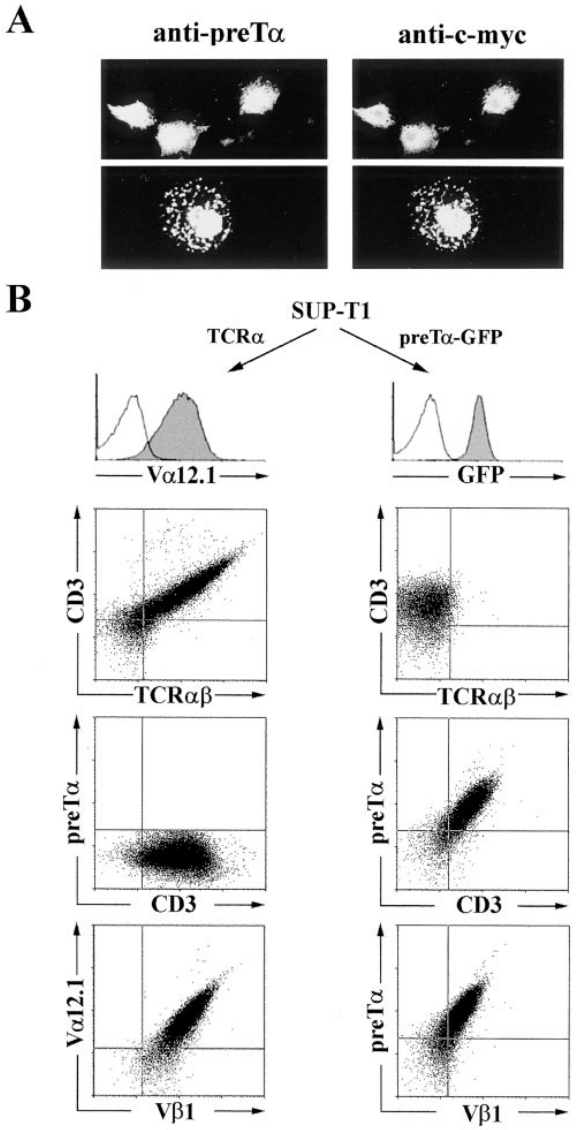

Figure 2. Specificity of anti-pTα ED-1 antiserum by immunofluorescence microscopy and flow cytometric analysis of pTα transfectants. (*A*) COS cells were transfected with a human pTα cDNA tagged with a c-myc epitope. After fixation and permeabilization, cells were sequentially stained with the affinity-purified anti-pTα ED-1 rabbit antiserum and the 9E10 anti–c-myc mAb. FITC-coupled goat anti–rabbit Ig and Texas red–coupled goat anti–mouse IgG were used as second Abs, respectively. Original magnification: ×400 (*top panels*) and ×630 (*bottom panels*). (*B*) SUP-T1 human T-lineage cells were transfected either with a productively rearranged human TCRα ($V_{\alpha}12.1$) cDNA or with a pTα-GFP cDNA. Stable transfectants characterized, respectively, as $V_{\alpha}12.1^{+}$ or GFP^{+} by flow cytometry (*shaded monoparametric histograms*) were assayed for their reactivity with anti-TCRα/β and anti-CD3 mAbs (*top biparametric histograms*), or with ED-1 anti-pTα antiserum and anti-CD3 (*middle histograms*). Coexpression of endogenous TCRβ chain (Vβ1) with either pTα or TCRα ($V_{\alpha}12.1$) was assayed on pTα-GFP and TCRα transfectants, respectively (*bottom histograms*). Background values were determined with preimmune rabbit serum and isotype-matched irrelevant mAbs.

pTα-GFP chimeric protein was used in these studies, reactivity of the anti-pTα antiserum could be analyzed by flow cytometry on stable transfectants traced by their GFP expression. As shown in Fig. 2 *B*, such GFP^{+} transfectants expressed low but detectable levels of CD3, but were unreactive with the BMA031 mAb which recognizes a common epitope of the TCRα/β dimer (22). In contrast, both TCRα/β and CD3 were detected on SUP-T1 clones stably transfected with a TCRα chain ($V_{\alpha12.1}$), whose expression could be followed with the anti-$V_{\alpha12.1}$ mAb 6D6 (25). Interestingly, a reciprocal expression pattern was observed when surface staining was performed with the anti-pTα Ab plus anti-CD3. Thus, pTα (GFP^{+}) transfectants, but not TCRα ($V_{\alpha12.1}{}^{+}$) transfectants, were reactive with the anti-pTα antiserum and coexpressed CD3 in stoichiometric amounts (Fig. 2 *B*). It is worth noting that expression of the endogenous TCRβ could be specifically detected with an anti-$V_{\beta1}$ mAb (24) on both cell types. Strikingly, levels of TCRβ expressed on $pT\alpha^{+}$ transfectants were consistently lower than those on TCRα-expressing clones, although in both cases, either pTα or TCRα was coexpressed with TCRβ in stoichiometric amounts (Fig. 2 *B*). As a whole, these data suggest that the ED-1 antiserum was able to specifically detect pTα-containing surface complexes which likely comprise CD3-associated TCRβ-pTα heterodimers, the hallmark of the pre-TCR complex.

Surface pTα Expression Is Restricted In Vivo to Large-sized $CD3^{low}$ TCRα/β^{-} DP Thymocytes. Having established that the anti-pTα antiserum recognized specifically pTα-containing surface complexes, we wished to examine whether pTα was actually expressed on the surface of TCRα/β^{-} primary thymocytes. To this end, Percoll-fractionated large and small DP thymocytes depleted of $CD3^{int}$ and $CD3^{bright}$ cells (including both TCRα/β^{+} and TCRγ/δ^{+} cells) were analyzed by flow cytometry for their reactivity with the anti-pTα Ab. As expected, both isolated DP cell subsets were exclusively composed of $CD3^{-}$ and $CD3^{low}$ cells (Fig. 3 *A*). $CD3^{low}$ thymocytes made up ~50 and 30% of the large- and small-sized DP thymocytes, respectively. Of these, only small $CD3^{low}$ thymocytes coexpressed the α/β TCR (see above), albeit at low levels, suggesting that they were representative of the developmental onset of TCRα/β expression. As shown in Fig. 3 *A*, such cells were unreactive with the anti-pTα Ab. Expression of pTα was negative as well on $CD3^{-}$ DP thymocytes, regardless of their cellular size. In contrast, essentially all large $CD3^{low}$ cells displayed a low but detectable reactivity with the anti-pTα Ab, thus providing direct evidence that pTα-containing complexes are expressed in vivo on the surface of normal pre-T cells. That this low level staining is specific was demonstrated by showing that it could be completely inhibited by the specific pTα peptide (Fig. 3 *B*). It is worth noting that pTα and CD3 were coexpressed on large $CD3^{low}$ thymocytes in a stoichiometric-like fashion similar to that observed on SUP-T1 pTα transfectants (Fig. 2 *B*), suggesting that the pTα-containing complex expressed on the former cells did correspond to the CD3-associated pre-TCR.

Developmental Status of Subsets of TCRα/β^{-} DP Thymocytes. The above results allowed a novel subdivision of the TCRα/β^{-} DP compartment into three individual subsets of thymocytes defined as large DP $CD3^{-}$, large DP $CD3^{low}$, and small DP $CD3^{-}$. Because pTα expression was

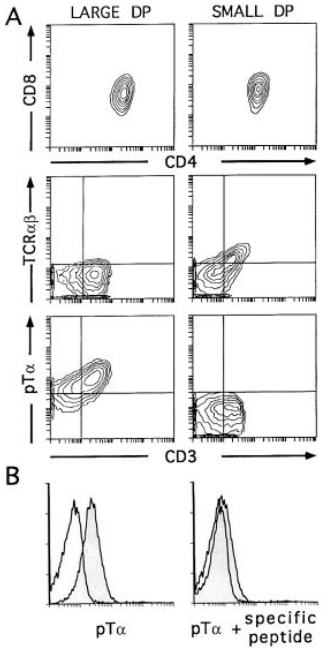

Figure 3. Analysis of surface pTα chain expression on normal human thymocytes. $CD4^+CD8^+$ DP cells were isolated from Percoll-separated large and small thymocytes after depletion of $CD3^{int}$ and $CD3^{bright}$ cells. (*A*) Each cell subset was independently analyzed by two-color flow cytometry for CD4 versus CD8 expression (*top panels*), and for their reactivity with anti-TCRα/β and anti-CD3 mAbs (*middle panels*), or with anti-pTα and anti-CD3 (*bottom panels*). Background values were obtained with preimmune rabbit serum and isotype-matched irrelevant mAbs. (*B*) Peptide competition assay. Large DP $TCR\alpha/\beta^-$ thymocytes were stained with ED-1 anti-pTα rabbit antiserum after PBS (*left*) or specific pTα peptide (*right*) incubation (*shaded areas*). *Unshaded areas*, Background fluorescence.

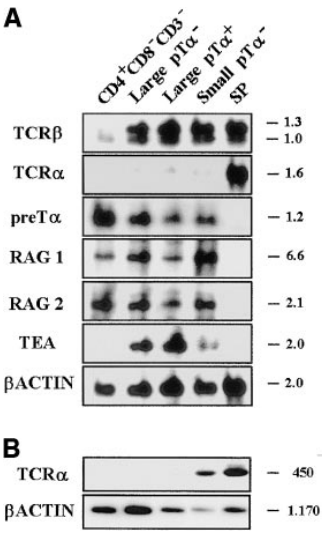

Figure 4. Analysis of transcriptional regulation of relevant genes involved in pre-T cell development. (*A*) Northern blots of total RNA isolated from the indicated populations were sequentially hybridized with the cDNA probes indicated (*left*). β-Actin mRNA expression served as internal control. (*B*) RT-PCR analysis of TCRα gene transcription. cDNA samples were amplified by using a pan-Vα primer in concert with a Cα-specific primer. Equivalence of cDNA among different samples was assessed by RT-PCR using β-actin primers under nonsaturating conditions. Sizes of the bands are indicated at the right (kb [*A*] or bp [*B*]).

restricted to large DP $CD3^{low}$ thymocytes, we wanted to investigate further the developmental status of the distinct $pT\alpha^+$ and $pT\alpha^-$ populations in order to improve definition of their precursor–product relationships. To this end, the three cell subsets were independently isolated and examined for their respective patterns of TCRβ, TCRα, and pTα gene expression. Northern blot analysis shown in Fig. 4 *A* revealed that both the 1.3-kb mature and the 1.0-kb immature TCRβ transcripts were expressed in the three subsets of $TCR\alpha/\beta^-$ DP thymocytes, regardless of their cellular size and CD3 phenotype. In contrast, TCRα transcription was undetectable in all of them, but occurred at high levels in mature SP thymocytes included as control. As expected, $CD4^+CD8^-CD3^-$ cells, which represent upstream precursors of the $TCR\alpha/\beta^-$ DP thymocyte pool as a whole (15), lacked both TCRβ and TCRα mature transcripts, but expressed 1.0-kb TCRβ mRNA. Therefore, we concluded that the three $TCR\alpha/\beta^-$ DP subsets identified in this study include cells that have already completed TCRβ, but not TCRα, gene rearrangement and transcription, indicating that they represent discrete pre-T cell stages along the pathway of T cell development. As expected of pre-T cells, all three cell types expressed pTα mRNA, with higher levels in the large $CD3^-$ subset. Maximal pTα expression was found in the more immature $CD4^+CD8^-CD3^-$ thymocytes (Fig. 4 *A*). A more sensitive RT-PCR analysis of these very same populations confirmed the patterns of TCRβ and pTα expression obtained by Northern blotting (not shown). However, it revealed that TCRα transcription had occurred, albeit at low levels, in small $CD3^-$ thymocytes, whereas it was completely absent from both the $CD3^-$ and the $CD3^{low}$ subsets of large pre-T cells (Fig. 4 *B*). Based on these results, we concluded that small DP $CD3^-$ thymocytes represented the particular stage at which TCRα gene rearrangement and transcription are initiated during human T cell development; therefore, this subset was placed at the latest pre-T cell stage, downstream of both subsets of large pre-T cells.

Additional support for the proposed model came from studies aimed at investigating the TEA and RAG gene transcription patterns displayed by the three pre-T cell subsets. TEA is a TCRα germline transcript whose expression seems to be an obligatory early event in the opening of the TCRα locus for subsequent rearrangement (17). As Vα to Jα recombination necessarily involves deletion of the TEA region (17), we reasoned that the onset of TCRα gene expression should necessarily be accompanied by a reciprocal shutdown of TEA transcription. Northern blot analysis performed with a specific TEA probe generated in this study revealed that TEA transcription had not been induced in early $CD4^+CD8^-CD3^-$ thymocytes, but occurred at high levels in large $CD3^-$ DP thymocytes, and was maximal in $pT\alpha^+$ pre-T cells (Fig. 4 *A*). However, it was sharply downregulated in small $CD3^-$ thymocytes, thus supporting the notion that the onset of TCRα gene expression concurs with a decrease in TEA transcription, these being coincident events in the transition from large to small pre-T cells. A reciprocal pattern of RAG gene expression was observed at this developmental point after hybridization with RAG-1– and RAG-2–specific probes (Fig. 4 *A*). Thus, although RAG-1 and RAG-2 transcripts were detected at similarly high levels in $CD4^+CD8^-CD3^-$ and large DP $CD3^-$ thymocytes, their expression was five- to eightfold lower in $pT\alpha^+$ pre-T cells. Interestingly, maximal transcription levels of both genes corresponded to small $CD3^-$ pre-T cells. These results suggest that RAG gene expression is selectively turned down in pre-TCR–expressing pre-T cells, and is later regained in small pre-T cells, allowing rearrangements at the TCRα locus to occur.

TCRβ Chain Expression and Cell Cycle Analysis of Subsets of Pre-T Cells. Formation and expression of the pre-TCR is claimed to immediately promote a cell cycle transition, which results in expansion and selection (β-selection) of the pool of pre-T cells deemed useful by virtue of successful

TCRβ chain expression (1, 11). Therefore, the prediction would be that all cells downstream of the pre-TCR–expressing pre-T cell stage should show evidence of β-selection. To address this issue, pre-T cell subsets were independently analyzed by flow cytometry for their DNA content as well as expression of cytoplasmic TCRβ protein. Results shown in Fig. 5 *A* revealed that essentially all (>90%) large $pT\alpha^+$ as well as small $CD3^-$ pre-T cells expressed cytoplasmic TCRβ; therefore, both cell subsets comprise β-selected pre-T cells. Unexpectedly, however, only 50–80% of large $CD3^-$ DP thymocytes (50% in this particular experiment) expressed cytoplasmic TCRβ, whereas the remaining 30–50% were $TCR\beta^-$. Such a differential expression of cytoplasmic TCRβ defined two distinct cell subsets of large $CD3^-$ pre-T cells which could thus be placed on either side of the β-selection process.

Formal support for this notion came from additional flow cytometric studies that addressed directly the cell cycle status of either the $TCR\beta^+$ or the $TCR\beta^-$ subsets of large $CD3^-$ pre-T cells. As shown in Fig. 5 *B*, double staining with anti-TCRβ and PI demonstrated that essentially all (>90%) large $CD3^-$ pre-T cells lacking TCRβ were arrested in the G_0/G_1 phase of the cell cycle, whereas, as expected of β-selected thymocytes, $TCR\beta^+$ $CD3^-$ pre-T cells featured a high proportion (up to 55%) of cells in $S/G_2/M$. This is consistent with 30% of bulk $CD3^-$ pre-T cells being in $S/G_2/M$ (Fig. 5 *A*). Therefore, $TCR\beta^-$ large pre-T cells are strong candidates for cells immediately before β-selection, and most likely immediately downstream of the $CD4^+CD8^-CD3^-$ precursor stage, which was essentially composed of $TCR\beta^-$ thymocytes (>95%) displaying only a background level (<10%) of cells in $S/G_2/M$ (Fig. 5 *A*). As expected of β-selected thymocytes, large $pT\alpha^+$ pre-T cells were highly enriched in cycling cells (~55% in $S/G_2/M$). However, TCRβ expression could not be associated with an active cycling state in small $CD3^-$ pre-T cells. Rather, these cells typically displayed only background levels of cells in $S/G_2/M$ (<15%), with a substantial fraction of them (>50%) in the G_2/M phase (Fig. 5 *A*). As an additional indicator of their resting state, small $CD3^-$ pre-T cells were shown to display exclusively the fast hypophosphorylated form of retinoblastoma (not shown). We thus concluded that most, if not all, small $CD3^-$ DP thymocytes are noncycling pre-T cells that have already passed through β-selection. This, in turn, suggests that β-selected large pre-T cells may normally lose surface pre-TCR expression and return to slow cycle conditions before the onset of TCRα gene expression. As a whole, these data provide strong evidence that small resting pre-T cells represent the latest pre-T cell stage in human thymocyte development, immediately upstream of conventional DP $TCR\alpha/\beta^+$ resting thymocytes.

Small $CD3^-$ Pre-T Cells Are Functional Intermediates between Large $CD3^{low}$ Pre-T Cells and $TCR\alpha/\beta^+$ DP Thymocytes. To seek direct evidence that small $CD3^-$ DP thymocytes represent the normal progeny of large pre-TCR–expressing pre-T cells in the pathway of T cell differentiation, highly purified large $CD3^{low}$ pre-T cells (>98% pure) were analyzed for their developmental fate in a hybrid hu/mo FTOC system. The pattern of differentia-

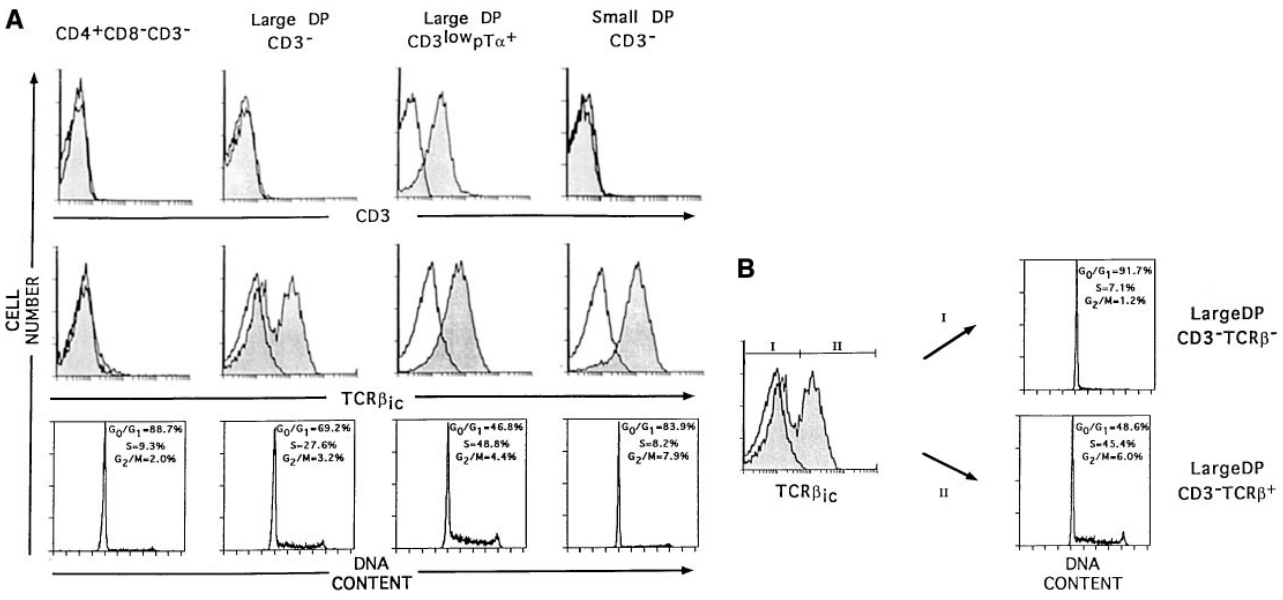

Figure 5. Intracytoplasmic TCRβ chain expression and DNA content analysis of $TCR\alpha/\beta^-$ thymocyte subsets. (*A*) Flow cytometry analysis of CD3 surface expression (*top panels*) or intracytoplasmic (*ic*) TCRβ (βF1) expression (*middle panels*) of $CD4^+CD8^-CD3^-$, large DP $CD3^-$, large DP $CD3^{low}pT\alpha^+$, and small DP $CD3^-$ thymocytes isolated as described in Materials and Methods (*shaded histograms*). *Unshaded histograms*, Background fluorescence. Cells from each subset were analyzed for DNA content by flow cytometry after staining with PI. Doublet discrimination ensured that only single cells were counted. Percentages of cells in G_0/G_1, S, and G_2/M are indicated (*bottom panels*). (*B*) Two-color flow cytometry analysis of TCRβ chain expression versus DNA content of large DP $CD3^-$ thymocytes. Cells were electronically gated based on intracytoplasmic (*ic*) TCRβ chain expression (*I*, $TCR\beta^-$; *II*, $TCR\beta^+$) and reanalyzed for DNA content.

tion from several experiments was identical (Fig. 6 *A*): the rapid appearance of $CD3^-$ DP cells (up to 60% by day 5 in this experiment) with minimal differentiation into $TCR\alpha/\beta^+$ cells (>5%), followed by the generation of a major population of conventional DP thymocytes that coexpressed CD3 and the α/β TCR at low to intermediate levels (85% by day 17), and the later appearance of small numbers of mature SP thymocytes (not shown). FSC analysis of the cells harvested on day 5 in the experiment shown in Fig. 6 *A* revealed that, by this stage, the cells that remained $CD3^{low}$ had kept their original size, whereas the $CD3^-$ cells generated in the lobes were significantly smaller (mean FSC: 450 vs. 410, respectively). However, by day 17, essentially all large cells had reverted to small cells, and thus, all $TCR\alpha/\beta^+$ progeny generated by this time (85%) were similar in size to the remaining (15%) $CD3^-$ DP cells (mean FSC: 330, 335, and 329, for $CD3^-$, $TCR\alpha/\beta^{low}$, and $TCR\alpha/\beta^{int}$ cells, respectively). Interestingly, total yields of viable human cells increased progressively during the initial phase of culture, resulting in a 15–20-fold increase of absolute cell numbers by days 5–7, but cellular recoveries then stabilized or increased modestly (up to 2–3 times) through the next 10–12 d, and declined steadily thereafter.

The above data indicate that cell division in thymus lobes reconstituted with large $CD3^{low}$ pre-T cells is extensive and skewed to the early stages of culture. Therefore, the high yields of $TCR\alpha/\beta^+$ DP progeny in FTOC are mostly a reflection of cellular expansion of blast precursors, presumably before transition to small $CD3^-$ pre-T cells. This in turn suggests that differentiation into $TCR\alpha/\beta^+$ DP cells can occur in the absence of cell division from small noncycling $CD3^-$ pre-T cells. To provide direct evidence of precursor activity, we tested the capacity of highly purified (>98%) populations of small $CD3^-$ DP thymocytes to produce $TCR\alpha/\beta^+$ progeny in the FTOC system. As shown in Fig. 6 *B*, a high proportion of both $TCR\alpha/\beta^{low}$ (20%) and $TCR\alpha/\beta^{int}$ (50%) progeny was already seen in the thymic lobes at day 1, the earliest sampling time. However, the number of $TCR\alpha/\beta^+$ progeny did not increase in absolute terms thereafter, an expected finding considering that all cells recovered by day 1 were small-sized cells (mean FSC: 300, 293, and 290, for $CD3^-$, $TCR\alpha/\beta^{low}$, and $TCR\alpha/\beta^{int}$ cells, respectively). Thus, although kinetics of $TCR\alpha/\beta^+$ cell generation were more pronounced with small $CD3^-$ than with large $CD3^{low}$ pre-T cells, total cell yields were substantially lower with the small $CD3^-$ pre-T cell fraction. Based on the above results, we concluded that small $CD3^-$ DP thymocytes represent functional intermediates between large pre-T cells and $TCR\alpha/\beta^+$ DP thymocytes.

Discussion

Considerable progress has recently been made in defining the role that preantigen receptors, namely the pre-B cell receptor and the pre-TCR, play in lymphocyte development. It is now established that both receptors direct in an analogous way the survival, expansion, and clonality of pre-B and pre-T lymphocytes by triggering cell cycle activation and the simultaneous downregulation of RAG genes (10, 11). However, less is known about the mechanisms that control terminal differentiation of lymphocyte precursors thus selected, especially in the T cell lineage. This can be partly attributed in both mice and humans to the lack of experimental data concerning regulation of pre-TCR expression on the surface of primary thymocytes, a fact that

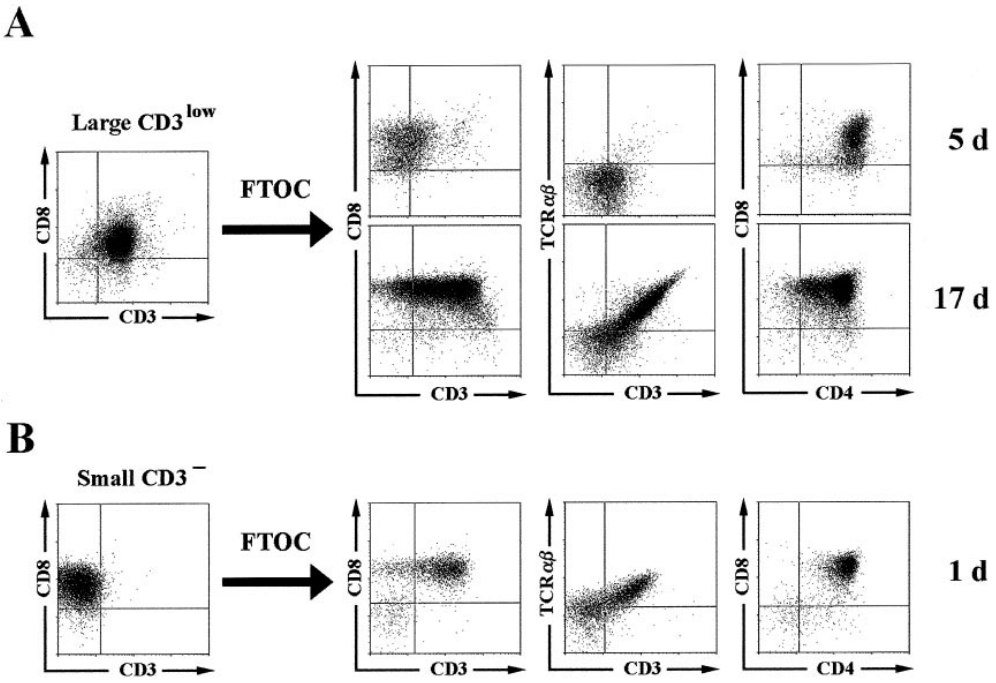

Figure 6. Phenotypic analysis of the cellular progeny generated after differentiation of large $CD3^{low}$ and small $CD3^-$ pre-T cells in a hybrid hu/mo FTOC. Large $CD3^{low}$ (*A*) and small $CD3^-$ (*B*) DP thymocytes, isolated as described in Materials and Methods, were analyzed by three-color flow cytometry after the indicated days of culture. Phenotypic analyses were performed on electronically gated human cells characterized as $CD45^+$ (not shown). Background fluorescence was determined by staining with isotype-matched irrelevant mAbs.

has hampered the definition of the developmental stages involved in the transition from TCRβ to TCRα rearrangement. In this study, analysis performed with a polyclonal rabbit Ab that recognizes an exposed epitope of the native human pTα protein has provided evidence for a restricted pattern of surface pTα expression during normal T cell development in humans. Surface pTα versus CD3 expression, together with cell cycle analyses, enabled a novel subdivision of the whole compartment of TCRβ-expressing pre-T cells into three distinct subsets of increasing maturity, and allowed the identification of a late stage of small noncycling pre-T cells representing the immediate precursors of TCRα/β-bearing thymocytes. The definition of the precursor–product relationships between such pre-T cell subsets, together with the characterization of the stage-specific events associated with the developmental onset of TCRα gene expression, namely exit from cell cycle, reexpression of RAG genes, and downregulation of TCRα germline transcription, collectively support the developmental scheme depicted in Fig. 7.

The distinct pre-T cell stages defined in our model are all included within a subset of $CD4^+CD8^+$ DP thymocytes that lack the mature α/β TCR and represent, as a whole, the downstream progeny of $CD4^+CD8^-CD3^-$ thymocyte precursors (15). About one third of such DP $TCR\alpha/\beta^-$ thymocytes are larger in size than the remaining two thirds and, thus, the two cell types have been defined, respectively, as large and small pre-T cells. Although pTα transcription is common to all pre-T cell stages, surface expression of the pTα protein is shown to be restricted to a limited fraction (50%) of large-sized pre-T cells that coexpress small but stoichiometric amounts of CD3. As neither pTα nor CD3 is detectable on the rest of the large and small pre-T cells, the coexpression of both molecules seems to define the particular subset of primary pre-T cells in which the pTα chain is paired with TCRβ and associates with CD3 to form the pre-TCR. However, attempts to demonstrate coexpression of surface TCRβ in vivo were unsuccessful, essentially because neither anti-TCRβ mAbs useful for flow cytometry nor anti-pTα reagents suitable for biochemical studies are yet available. Despite this, the possibility that TCRβ-pTα heterodimers associated with CD3 are indeed expressed on $pT\alpha^+$ pre-T cells is strongly supported by several independent findings: (*a*) low but stoichiometric amounts of pTα and CD3 were specifically coexpressed with endogenous TCRβ on pTα transfectants derived from a TCRα-deficient cell line; (*b*) we have previously shown that heterodimeric complexes containing TCRβ without TCRα could be immunoprecipitated from unfractionated large DP $TCR\alpha/\beta^-$ thymocytes (15); (*c*) others have noticed that large thymocytes from TCRα-deficient and TCRβ transgenic RAG-1 mutant mice express low but stoichiometric amounts of surface TCRβ and CD3 (13), similar to what has been reported for mouse thymocytes from which a CD3-associated pTα-TCRβ heterodimeric complex has recently been characterized (14); and (*d*) to date, no surface pTα expression has been described without association with TCRβ and CD3.

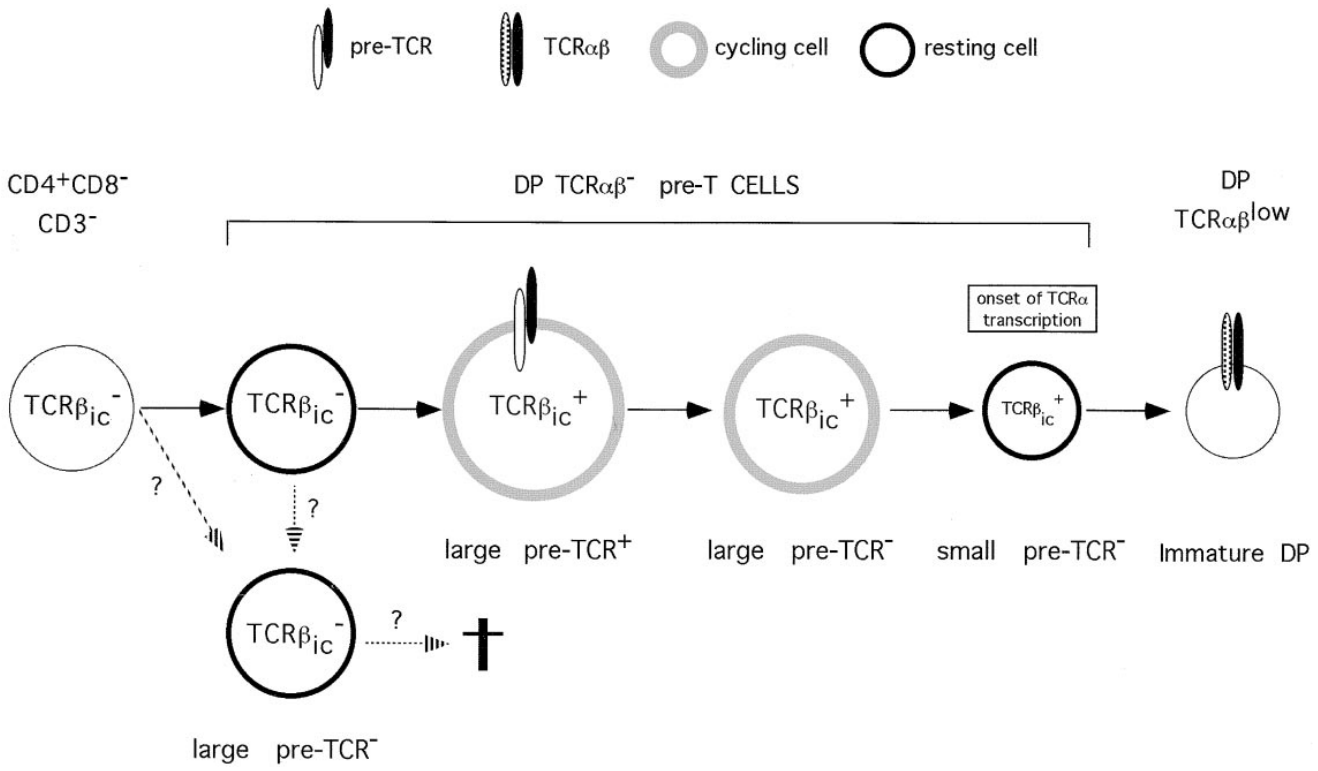

Figure 7. Proposed model of pre-T cell development in the human thymus. *ic*, Intracytoplasmic.

Therefore, expression of surface pre-TCR complexes is proposed in our model to be confined to the minor subset of large $pT\alpha^+$ $CD3^{low}$ pre-T cells, whereas large pre-T cells lacking detectable amounts of surface pTα and CD3 (~50% of all large DP $TCR\alpha/\beta^-$ thymocytes) are proposed to be homogeneously negative for pre-TCR expression (Fig. 7). However, the latter cells represent a heterogeneous population in which a major fraction (50–80%) have already passed β-selection, as indicated by their high expression levels of intracellular TCRβ (11), whereas the remaining cells (20–50%) still lack cytoplasmic TCRβ and may thus represent intermediates between $CD4^+CD8^-CD3^-$ thymocytes and the first β-selected pre-T cells. It is highly likely that such intermediates include the pool of precursor thymocytes undergoing rearrangements at the TCRβ locus, although they may also include cells carrying nonproductive Vβ-Dβ-Jβ joints on both TCRβ loci, which may thus be destined to die. Both possibilities, illustrated in Fig. 7, are compatible with the hypothesis that the human pre-TCR does not participate, as does its murine counterpart, in the transition to the DP stage (2, 3, 18). Rather, expression of CD8 appears to precede pre-TCR expression during human T cell development.

An important aspect of our study was the observation that virtually all large pre-T cells with cytoplasmic TCRβ, whether or not they display surface pTα chain expression, were actively engaged in cell cycle, a characteristic previously associated with the process of β-selection (11). Conversely, DP thymocytes lacking TCRβ protein were nondividing cells arrested at G_0/G_1. The finding that up to 40% of cycling, β-selected pre-T cells did not express the putative pre-TCR is apparently difficult to reconcile with the current idea that cell cycle activation involves signaling mediated through the pre-TCR (2, 3, 11). However, the possibility that undetectable, but functional, amounts of the pre-TCR are expressed on the surface of such cycling $pT\alpha^-$ pre-T cells cannot be formally excluded. Alternatively, it is likely that, as proposed for pre-B cells at the equivalent developmental point (35), β-selected pre-T cells rapidly downregulate expression of the pre-TCR from the cell surface while they are still in cycle. In this latter situation, it could be expected that the maintained expression of surface pre-TCR in a short developmental window is both necessary and sufficient to provide a sustained proliferation signal that would allow pre-T cells to undergo a great cellular expansion before turning back to slow cycle conditions. Supporting this hypothesis, results from a recent study have provided evidence that such a proliferation phase corresponds in mice to nine rapid cell divisions that last for ~4 d and end at the small resting DP thymocyte stage (36). This concurs with our finding that a major fraction (about two thirds) of β-selected pre-TCR^- pre-T cells in humans are small-sized, nondividing cells. Interestingly, although such small pre-T cells do not yet express the mature α/β TCR, they already transcribe low levels of the TCRα gene. Thus, they are proposed to define the developmental point at which onset of TCRα gene rearrangement and transcription occurs, and are placed in our model at the latest pre-T cell stage, immediately upstream of the first TCRα/β-expressing DP thymocytes (Fig. 7).

Consistent with the above proposal, we found that indicators of Vα-Jα recombinase activity, such as RAG gene reexpression and downregulation of TEA transcription, are coincident and stage-specific events induced after entry of late pre-T cells into the pool of small, resting cells. Thus, it was observed that expression of RAG genes, which is turned down after pre-TCR signaling (11, 18), is regained in small pre-T cells, allowing rearrangements at the TCRα locus to be initiated at this stage. Further, the demonstration that germline transcription of TCRα spans all cycling pre-T cell stages but drops significantly in resting pre-T cells also supports the concept that these cells are actively rearranging their Vα genes. Similarly, Ig L chain gene rearrangement is restricted to small, resting pre-B cells that represent the equivalent precursor stage along the B cell pathway (35). In contrast to the proposal that small resting TCR^- DP thymocytes are functional intermediates in the T cell differentiation pathway, it is currently assumed that these cells represent the large pool of end-stage products of failed rearrangement attempts. However, recently published data have shown that small noncycling TCR^- DP thymocytes in the mouse are actually the physiological targets of the multiple rearrangements that occur at the TCRα locus (20), and are subject to positive selection (21, 37). Direct evidence of the physiological relevance of small resting $CD3^-$ pre-T cells in humans was further provided by the demonstration that these cells are functional intermediates between large $pT\alpha^+$ pre-T cells and $TCR\alpha/\beta^+$ DP thymocytes. Accordingly, as shown previously in mice (19, 20), surface expression of the mature CD3–TCRα/β complex can be first detectable on small nonproliferating DP thymocytes.

As a whole, our results suggest that, after pre-TCR–mediated cellular expansion, β-selected large pre-T cells may normally downregulate surface pre-TCR expression and return to slow cycle conditions before the onset of TCRα gene expression. The proposed pattern of pre-TCR expression differs from previous hypothetical models in mice postulating that mature TCRα/β and pre-TCR complexes are coexpressed on the cell surface of late pre-T cells (10). However, it is still possible that some of these cells are cotranscribing pTα and TCRα genes. It is tempting to speculate that, in that situation, both molecules compete with each other for dimerization with TCRβ, the affinity of TCRα being higher than that of pTα. Alternatively, as proposed in mice, another still unknown component of the pre-TCR (i.e., the hypothetical VpreT) might be already shut off at the earliest $TCR\alpha^+$ stages, hence preventing surface expression of the whole pre-TCR complex (3). Finally, it must be stressed that the restricted pattern of surface pTα expression shown in this study closely resembles that of the surrogate light chain of the pre-B cell receptor (35, 38). This emphasizes the similarities of early developmental events associated with the transient expression of both preantigen receptors during T and B cell development.

We wish to thank Drs. B. Alarcón, M.A. Alonso, M. Brenner, R. Kurrle, J.A. López de Castro, T.W. Mak, and L.A. Turka for the generous gift of Abs and cDNAs, Dr. S.G. Copín for invaluable advice on the FTOC, and the Pediatric Cardiosurgery Units from the Centro Especial Ramón y Cajal and Ciudad Sanitaria La Paz (Madrid) for the thymus samples.

This work was supported in part by Glaxo Wellcome S.A., and by grants SAF95-0006 and SAF97-0161 from Comisión Interministerial de Ciencia y Tecnología (CICYT) and CAM083/013/97 from Comunidad de Madrid. We would also like to thank the Fundación Ramón Areces for an Institutional Grant to the Centro de Biología Molecular "Severo Ochoa." C. Trigueros and A.R. Ramiro are fellows of Fondo de Investigaciones Sanitarias and the Ministerio de Educación y Ciencia, respectively.

Address correspondence to María L. Toribio, Centro de Biología Molecular "Severo Ochoa," CSIC-UAM, Facultad de Biología, Universidad Autónoma de Madrid, Cantoblanco 28049, Madrid, Spain. Phone: 34-1-3978076; Fax: 34-1-3978087; E-mail: mtoribio@trasto.cbm.uam.es

Received for publication 17 November 1997 and in revised form 26 June 1998.

References

1. Dudley, E.C., H.T. Petrie, L.M. Shah, M.J. Owen, and A. Hayday. 1994. T cell receptor β chain gene rearrangement and selection during thymocyte development in adult mice. *Immunity*. 1:83–93.
2. Levelt, C.N., and K. Eichmann. 1995. Receptors and signals in early thymic selection. *Immunity*. 3:667–672.
3. von Boehmer, H., and H.J. Fehling. 1997. Structure and function of the pre-T cell receptor. *Annu. Rev. Immunol*. 15: 433–452.
4. Saint-Ruf, C., K. Ungewiss, M. Groettrup, L. Bruno, H.J. Fehling, and H. von Boehmer. 1994. Analysis and expression of a cloned pre-T cell receptor gene. *Science*. 266:1208–1212.
5. Groettrup, M., K. Ungewiss, O. Azogui, R. Palacios, M.J. Owen, A.C. Hayday, and H. von Boehmer. 1993. A novel disulfide-linked heterodimer on pre-T cells consists of the T cell receptor β chain and a novel 33 kd glycoprotein. *Cell*. 75:283–294.
6. Fehling, H.J., A. Krotkova, C. Saint-Ruf, and H. von Boehmer. 1995. Crucial role of the pre-T-cell receptor α gene in development of αβ but not γδ T cells. *Nature*. 375:795–798.
7. Jacobs, H., J. Iacomini, M. van den Ven, S. Tonegawa, and A. Berns. 1996. Domains of the TCRβ-chain required for early thymocyte development. *J. Exp. Med*. 184:1833–1843.
8. O'Shea, C.C., A.P. Thornell, I.R. Rosewell, B. Hayes, and M.J. Owen. 1997. Exit of the pre-TCR from the ER/*cis*-Golgi is necessary for signaling differentiation, proliferation, and allelic exclusion of immature thymocytes. *Immunity*. 7: 591–599.
9. Irving, B.A., F.W. Alt, and N. Killeen. 1998. Thymocyte development in the absence of pre-T cell receptor extracellular immunoglobulin domains. *Science*. 280:905–908.
10. Borst, J., H. Jacobs, and G. Brouns. 1996. Composition and function of T-cell receptor and B-cell receptor complexes on precursor lymphocytes. *Curr. Opin. Immunol*. 8:181–190.
11. Hoffman, E.S., L. Passoni, T. Crompton, T.M.J. Leu, D.G. Schatz, A. Foff, M.J. Owen, and A.C. Hayday. 1996. Productive T-cell receptor β-chain gene rearrangement: coincident regulation of cell cycle and clonality during development in vivo. *Genes Dev*. 10:948–962.
12. Wilson, A., and H.R. MacDonald. 1995. Expression of genes encoding the pre-TCR and CD3 complex during thymus development. *Int. Immunol*. 7:1659–1664.
13. Mombaerts, P., S.J. Anderson, R.G. Perlmutter, T.W. Mak, and S. Tonegawa. 1994. An activated *lck* transgene promotes thymocyte development in RAG-1 mutant mice. *Immunity*. 1:261–267.
14. Berger, M.A., V. Davé, M.R. Rhodes, G.C. Bosma, M.J. Bosma, D.J. Kappes, and D.L. Wiest. 1997. Subunit composition of pre-T cell receptor complexes expressed by primary thymocytes: CD3δ is physically associated but not functionally required. *J. Exp. Med*. 186:1461–1467.
15. Ramiro, A.R., C. Trigueros, C. Márquez, J.L. San Millán, and M.L. Toribio. 1996. Regulation of pre-T cell receptor (pTα-TCRβ) gene expression during human thymic development. *J. Exp. Med*. 184:519–530.
16. Wilson, A., W. Held, and H.R. MacDonald. 1994. Two waves of recombinase gene expression in developing thymocytes. *J. Exp. Med*. 179:1355–1360.
17. Wilson, A., J.P. de Villartay, and H.R. McDonald. 1996. T cell receptor γ gene rearrangement and T early α (TEA) expression in immature αβ lineage thymocytes: implications for αβ/γδ lineage commitment. *Immunity*. 4:37–45.
18. Levelt, C.N., B. Wang, A. Ehrfeld, C. Terhorst, and K. Eichmann. 1995. Regulation of T cell receptor (TCR)-β locus allelic exclusion and initiation of TCR-α locus rearrangement in immature thymocytes by signaling through the CD3 complex. *Eur. J. Immunol*. 25:1257–1261.
19. Petrie, H.T., M. Pearse, R. Scollay, and K. Shortman. 1990. Development of immature thymocytes: initiation of CD3, CD4, and CD8 acquisition parallels down-regulation of the interleukin-2 receptor α chain. *Eur. J. Immunol*. 20:2813–2816.
20. Petrie, H.T., F. Livak, D.G. Schatz, A. Strasser, I.N. Crispe, and K. Shortman. 1993. Multiple rearrangements in the T cell receptor α chain genes maximize the production of useful thymocytes. *J. Exp. Med*. 178:615–622.
21. Ernst, B., C.D. Surh, and J. Sprent. 1995. Thymic selection and cell division. *J. Exp. Med*. 182:961–972.
22. Borst, J., J.J.M. van Dongen, E. de Vries, W.M. Comans-Bitter, M.J.D. van Tol, J.M. Vossen, and R. Kurrle. 1990. BMA031, a monoclonal antibody suited to identify the T-cell receptor αβ/CD3 complex on viable human T lymphocytes in normal and disease states. *Hum. Immunol*. 29:175–188.
23. Band, H., F. Hochstenbach, J. McLean, S. Hata, M.S. Krangel, and M.B. Brenner. 1987. Immunochemical proof that a novel rearranging gene encodes the T cell receptor δ subunit.

Science. 238:682–684.
24. Posnett, D.N. 1996. First human TCR monoclonal antibody workshop. *The Immunologist*. 4:5–8.
25. DerSimonian, H., H. Band, and M.B. Brenner. 1991. Increased frequency of T cell receptor Vα12.1 expression on $CD8^+$ T cells: evidence that Vα participates in shaping the peripheral T cell repertoire. *J. Exp. Med.* 174:639–648.
26. Brenner, M.B., J. McLean, H. Scheft, R.A. Warnke, N. Jones, and J.L. Strominger. 1987. Characterization and expression of the human αβ T cell receptor by using a framework monoclonal antibody. *J. Immunol*. 138:1502–1509.
27. Mallabiabarrena, A., M.A. Jiménez, M. Rico, and B. Alarcón. 1995. A tyrosine-containing motif mediates ER retention of CD3-ϵ and adopts a helix-turn structure. *EMBO (Eur. Mol. Biol. Organ.) J.* 14:2257–2268.
28. Barber, D.F., D. López, and J.A. López de Castro. 1995. T cell receptor diversity in alloreactive responses against HLA-B27 (B*2705) is limited by multiple-level restriction in both α and β chains. *Eur. J. Immunol.* 25:2479–2485.
29. Yanagi, Y., A. Chan, B. Chin, M. Minden, and T.W. Mak. 1985. Analysis of cDNA clones specific for human T cells and the α and β chains of the T cell receptor heterodimer from a human T cell line. *Proc. Natl. Acad. Sci. USA*. 82:3430–3434.
30. Yoshikai, Y., D. Anatoniou, S.P. Clark, Y. Yanagi, R. Sangster, P. van den Elsen, C. Terhorst, and T.W. Mak. 1984. Sequence and expression of transcripts of the human T-cell receptor β-chain genes. *Nature*. 312: 521–524.
31. Turka, L.A., D.G. Schatz, M.A. Oettinger, J.J.M. Chun, C. Gorka, K. Lee, W.T. McCormack, and C.B. Thompson. 1991. Thymocyte expression of RAG-1 and RAG-2: termination by T-cell receptor cross-linking. *Science*. 253:778–781.
32. Broeren, C.P., G.M. Verjans, W. Van Eden, J.G. Kusters, J.A. Lenstra, and T. Logtenberg. 1991. Conserved nucleotide sequences at the 5′ end of T cell receptor variable genes facilitate polymerase chain reaction amplification. *Eur. J. Immunol*. 21:569–575.
33. Fisher, A.G., L. Larsson, L.K. Goff, D.E. Restall, L. Happerfield, and M. Merkenschlager. 1990. Human thymocyte development in organ cultures. *Int. Immunol.* 2:571–578.
34. Reynolds, T.C., S.D. Smith, and J. Sklar. 1987. Analysis of DNA surrounding the breakpoints of chromosomal translocations involving the beta T cell receptor gene in human lymphoblastic neoplasms. *Cell.* 50:107–117.
35. Rajewsky, K. 1996. Clonal selection and learning in the antibody system. *Nature*. 381:751–758.
36. Falk, I., J. Biro, H. Kohler, and K. Eichmann. 1996. Proliferation kinetics associated with T cell receptor-β chain selection of fetal murine thymocytes. *J. Exp. Med*. 184:2327–2339.
37. Lundberg, K., and K. Shortman. 1994. Small cortical thymocytes are subject to positive selection. *J. Exp. Med*. 179: 1475–1483.
38. Ghia, P., E. ten Boekel, E. Sanz, A. de la Hera, A. Rolink, and F. Melchers. 1996. Ordering of human bone marrow B lymphocyte precursors by single-cell polymerase chain reaction analyses of the rearrangement status of the immunoglobulin H and L chain gene loci. *J. Exp. Med.* 184:2217–2229.